

## Multicomponent solute transport model with cation exchange in a redox subsurface environment

**YOSHINARI HIROSHIRO, KENJI JINNO**

*Institute of Environmental Systems, Graduate School of Kyushu University, 6-10-1, Hakozaki, Higashi-ku, Fukuoka 812-8581, Japan*  
e-mail: [hirosiro@civil.kyushu-u.ac.jp](mailto:hirosiro@civil.kyushu-u.ac.jp)

**SHIN-ICHIRO WADA**

*Division of Bioresources and Environmental Sciences, Graduate School of Kyushu University, 6-10-1, Hakozaki, Higashi-ku, Fukuoka 812-8581, Japan*

**TAKUSHI YOKOYAMA**

*Department of Chemistry, Faculty of Science, Kyushu University, 6-10-1, Hakozaki, Higashi-ku, Fukuoka 812-8581, Japan*

**MOTOHIRO KUBOTA**

*Miyazaki Prefecture, 2-10-1, Tachibanadori-Higashi, Miyazaki 880-0805, Japan*

**Abstract** In order to clarify the behaviour of chemical species under reducing condition in a subaqueous soil similar to a paddy field, a column experiment was carried out. As Mn- and Fe-(hydr)oxides were dissolved by microbially mediated reduction,  $\text{Na}^+$ ,  $\text{K}^+$ ,  $\text{Mg}^{2+}$ ,  $\text{Ca}^{2+}$ ,  $\text{Mn}^{2+}$ , and  $\text{Fe}^{2+}$  existed in the pore water as major cations. The  $\text{Ca}^{2+}$  concentration had a tendency to decrease in the layer at 5–25 cm depth in the column, whereas the  $\text{Ca}^{2+}$  concentration increased with time below 45 cm depth. This phenomenon can be assumed to be due to the desorption of  $\text{Ca}^{2+}$ , by  $\text{Mn}^{2+}$  and  $\text{Fe}^{2+}$ , and its infiltration. Therefore, it is necessary to develop a solute transport model which takes into account both biochemical and cation exchange reactions. In this paper, a simulation model that considers both reactions is described and applied to simulate the results of the column experiment. The reliability of this model was evaluated by comparing the calculated results with the result of the experiment.

### INTRODUCTION

In recent years, strong demands have been made on multicomponent solute transport models in the subsurface environment. Since the behaviour of a chemical species under reducing conditions in subaqueous soils differs from that of a chemical species under oxidizing conditions, it is necessary to take into account the biochemical properties. In general, the soil matrix contains large amounts of Mn- and Fe-(hydr)oxides. Mn- and Fe-(hydr)oxides are dissolved by microbially-mediated reduction. As a consequence, it is considered that the cation exchange reaction takes place between  $\text{Na}^+$ ,  $\text{K}^+$ ,  $\text{Mg}^{2+}$ ,  $\text{Ca}^{2+}$  and  $\text{Mn}^{2+}$ ,  $\text{Fe}^{2+}$ . Accordingly, to clarify the behaviour of a chemical species under reducing conditions, it is necessary to develop a solute transport model which considers both the biochemical reaction and the cation exchange reaction.

Recently, different approaches for the simulation of transport processes involved in chemical reactions have been achieved (e.g. Rubin, 1983; Kinzelbach *et al.*, 1991;

Matsunaga *et al.*, 1993; Lensing *et al.*, 1994; Schäfer *et al.*, 1998a,b). For example, Kinzelbach *et al.* (1991) have developed a model describing microbial denitrification processes. Lensing *et al.* (1994) have modelled a biologically mediated redox process that includes Mn(IV)-reduction and Fe(III)-reduction. Schäfer *et al.* (1998a,b) have developed the reactive transport model TBC (Transport, Biochemistry, and Chemistry), which has been proved to be complex enough to grasp the important reactive processes. However, since Mn- and Fe-oxides are dissolved under reducing conditions, cation exchange reactions including  $Mn^{2+}$  and  $Fe^{2+}$  should also be considered in such models.

In this paper, to clarify the behaviour of chemical species under reducing conditions in subaqueous soils similar to a paddy field, a column experiment was carried out. A simulation model with cation exchange reaction was developed and the model was applied to simulate the results of the column experiment. The reliability of this model was evaluated by comparing the calculated and experimental results.

### CONCEPTUAL MODEL

The biochemical and chemical model (Fig. 1) describes the interaction of  $O_2$ ,  $NO_3^-$ ,  $CH_2O$ , bacteria, Mn-, Fe-(hydr)oxides,  $Na^+$ ,  $K^+$ ,  $Mg^{2+}$ , and  $Ca^{2+}$ . This model takes into account microbially-mediated redox reactions and the cation exchange. The bacteria are assumed to reside in an immobile biophase where all microbial activity takes place (Schäfer *et al.*, 1998a). The volume of the biophase is assumed to be constant in time and space and not coupled to bacterial growth.

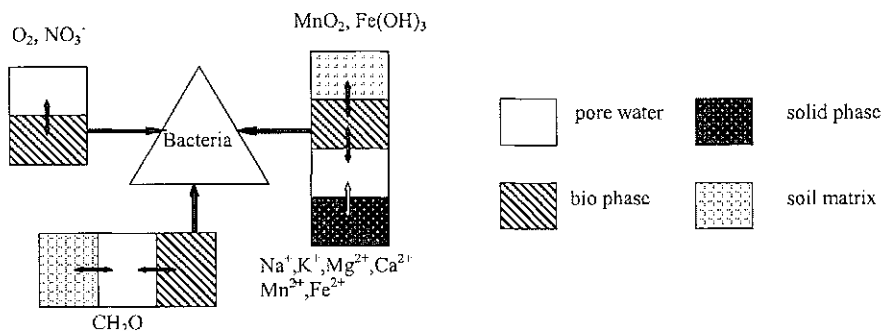


Fig. 1 Scheme of the biochemical model.

The mobile pore water, the biophase, the soil matrix, and the solid phase for cation exchange are considered as model phases. The solid phase for cation exchange is the immobile phase.

### REACTIVE SOLUTE TRANSPORT EQUATION

For this study, the chemical species considered are summarized in Table 1. The one-dimensional partial differential equation governing the convective-dispersive solute

**Table 1** Chemical species in the model.

Pore water	$\text{Na}^+_{mob}, \text{K}^+_{mob}, \text{Mg}^{2+}_{mob}, \text{Ca}^{2+}_{mob}, \text{Mn}^{2+}_{mob}, \text{Fe}^{2+}_{mob}, \text{O}_{2mob}, \text{NO}_3^-_{mob}, \text{CH}_2\text{O}_{mob}$
Solid phase	$\text{Na}^+_{im}, \text{K}^+_{im}, \text{Mg}^{2+}_{im}, \text{Ca}^{2+}_{im}, \text{Mn}^{2+}_{im}, \text{Fe}^{2+}_{im}$
Bio phase	$\text{O}_{2bio}, \text{NO}_3^-_{bio}, \text{MnO}_{2bio}, \text{Fe}(\text{OH})_3_{bio}, \text{CH}_2\text{O}_{bio}, \text{Mn}^{2+}_{bio}, \text{Fe}^{2+}_{bio}$
Bacteria	X1, X2, X3
Soil matrix	$\text{CH}_2\text{O}_{mat}, \text{MnO}_{2mat}, \text{Fe}(\text{OH})_3_{mat}$

transport of chemical species  $i$  considering biochemical and chemical reactions in a subaqueous soils can be written as (Bear, 1972):

$$\frac{\partial C_{mob(i)}}{\partial t} + v \frac{\partial C_{mob(i)}}{\partial z} - \frac{\partial}{\partial z} \left( D \frac{\partial C_{mob(i)}}{\partial z} \right) = S_{(i)} \quad i = 1, 2, \dots, N \quad (1)$$

where  $C_{mob(i)}$  is the concentration of chemical species  $i$  in the pore water [ $\text{mmol l}^{-1}$ ],  $v$  is pore water velocity [ $\text{cm s}^{-1}$ ],  $t$  is time [s],  $z$  is distance [cm],  $D$  is the hydrodynamic dispersion coefficient [ $\text{cm}^2 \text{s}^{-1}$ ],  $S_{(i)}$  is the chemical source-sink term representing the exchange with other phases and chemical or biochemical reactions [ $\text{mmol l}^{-1} \text{s}^{-1}$ ]. In our experiment,  $N$  is 9 and the chemical species given by  $i = 1, 2, 3, 4, 5, 6, 7, 8,$  and  $9$  correspond to  $\text{Na}^+_{mob}, \text{K}^+_{mob}, \text{Mg}^{2+}_{mob}, \text{Ca}^{2+}_{mob}, \text{Mn}^{2+}_{mob}, \text{Fe}^{2+}_{mob}, \text{O}_{2mob}, \text{NO}_3^-_{mob},$  and  $\text{CH}_2\text{O}_{mob}$ , respectively.

## CHEMICAL SOURCE-SINK TERMS

The chemical reaction term on the right-hand side of equation (1) is the source-sink term, which contains the biochemical reactions and the cation exchange reactions:

$$S = S1 + S2 + S3 \quad (2)$$

$$S1 = \frac{\alpha}{n_{mob}} ([C_{bio}] - [C_{mob}]) \quad (3)$$

$$S2 = \frac{\beta}{n_{mob}} ([C_{mat}] - [C_{mob}]) \quad (4)$$

$$S3 = - \frac{\partial [C_{im}]}{\partial t} \quad (5)$$

where  $S1$  is the term of exchange reaction at the concentration difference between the pore water and the biophase,  $S2$  is the term of exchange reaction at the concentration difference between the pore water and the soil matrix, and  $S3$  is the term of cation exchange reaction between the pore water and the solid phase. In equations (3), (4), and (5), the subscripts  $mob$ ,  $bio$ ,  $mat$ , and  $im$  correspond to the concentration of chemical species [ $\text{mmol l}^{-1}$ ] in the pore water, the biophase, the soil matrix, and the solid phase, respectively.  $\alpha$  and  $\beta$  are the exchange coefficients [ $\text{s}^{-1}$ ] and  $n_{mob}$  is the porosity.

## BACTERIA GROWTH

The general expression of Monod-type kinetics (equation (6)) is shown for one arbitrary bacteria group (Schäfer *et al.*, 1998a):

$$\left[ \frac{\partial X}{\partial t} \right]_{\text{growth}} = \sum v_{\max} \cdot X \cdot \prod_m MT_m \prod_i IT_i \quad (6)$$

$$MT_m = S_m / (MC_m + S_m) \quad (7)$$

$$IT_i = IC_i / (IC_i + S_i) \quad (8)$$

$$\left[ \frac{\partial X}{\partial t} \right]_{\text{decay}} = -v_{\text{dec}} \cdot X \quad (9)$$

where  $X$  is the bacteria population,  $v_{\max}$  is the maximum growth rate of bacteria,  $MT_m$  is the Monod terms for species  $m$ ,  $S_m$  is the concentration of species in biophase,  $MC_m$  is the Monod constant for species  $m$ ,  $IT_i$  is the inhibition term of the inhibiting species  $i$ ,  $IC_i$  is the inhibition constant,  $S_i$  is the inhibition concentration, and  $v_{\text{dec}}$  is the constant of bacteria decay rate.

The change of the  $\text{CH}_2\text{O}$  concentration in the biophase is linked to the bacteria growth and the consumption of the organic materials:

$$\left[ \frac{\partial [\text{CH}_2\text{O}_{\text{bio}}]}{\partial t} \right] = \sum_{i=1}^3 \left( \frac{1}{Y_{\text{OC}}} \left[ \frac{\partial X_i}{\partial t} \right]_{\text{growth}} - f_{\text{USE}} \left[ \frac{\partial X_i}{\partial t} \right]_{\text{decay}} \right) - \frac{\alpha}{n_{\text{bio}}} ([\text{CH}_2\text{O}_{\text{bio}}] - [\text{CH}_2\text{O}_{\text{mob}}]) \quad (10)$$

where  $f_{\text{USE}}$  is the utilizable coefficient of dead bacteria.

The consumption of electron acceptors  $\text{O}_2$  is related to the stoichiometric relations. The concentration change of mobile  $\text{O}_2$  in the biophase is:

$$\left[ \frac{\partial [\text{O}_{2\text{bio}}]}{\partial t} \right] = - \frac{1}{U_{\text{EA}}} \left[ \frac{\partial X}{\partial t} \right]_{\text{growth}}^{\text{aerobic}} - \frac{\alpha}{n_{\text{bio}}} ([\text{O}_{2\text{bio}}] - [\text{O}_{2\text{mob}}]) \quad (11)$$

$$U_{\text{EA}} = ST \cdot Y_{\text{OC}} / (1 - Y_{\text{OC}})$$

where  $ST$  is the stoichiometric coefficient. For solid electron acceptors (e.g.  $\text{MnO}_2$ ,  $\text{Fe}(\text{OH})_3$ ) and the exchange term in equation (11) is:

$$- \frac{\gamma}{n_{\text{bio}}} ([\text{MnO}_{2\text{bio}}] - [\text{MnO}_{2\text{mat}}]) \quad (12)$$

where  $\gamma$  is the exchange coefficient [ $\text{s}^{-1}$ ].

The release of the Mn- or the Fe-(hydr)oxides is related to bacteria growth, e.g. for Mn-(hydr)oxides, if  $P_{\text{Mn}^{2+}}$  is the production factor:

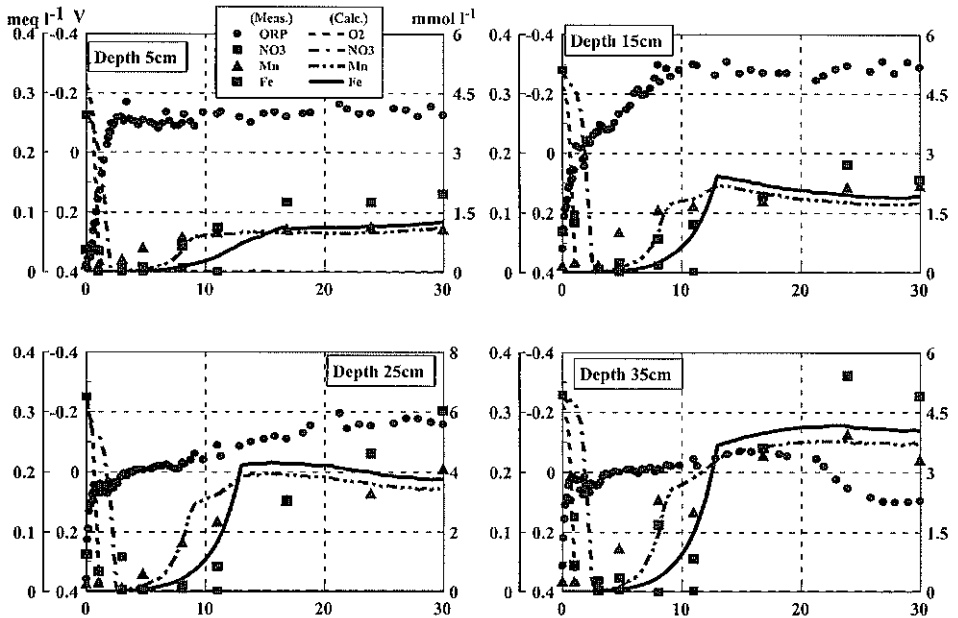
$$\left[ \frac{\partial [\text{Mn}^{2+\text{bio}}]}{\partial t} \right] = \frac{1}{P_{\text{Mn}^{2+}}} \left[ \frac{\partial X}{\partial t} \right]_{\text{growth}} - \frac{\alpha}{n_{\text{bio}}} ([\text{Mn}^{2+\text{bio}}] - [\text{Mn}^{2+\text{mob}}]) \quad (13)$$

## RESULTS

The biochemical and the transport parameters for the column simulation are shown in Table 2. Figure 2 shows the temporal variation in the concentrations of chemical species and the ORP (oxidation reduction potential) value. As can be seen in Fig. 2, the ORP values rapidly decreased and a reduction in the column was found to proceed. The calculated concentration of O<sub>2</sub> rapidly decreased at every depth about for first two days, thereafter, showed about zero. The variation of the calculated concentration of O<sub>2</sub> was nearly in accordance with the measured value of the ORP which rapidly decreased after approximately two days at the beginning of the experiment. The calculated concentration of NO<sub>3</sub> was able to be approximately reproduced compared to the variation of the measured concentration. In order to fit the measured and the calculated concentrations of O<sub>2</sub> and NO<sub>3</sub>, it was confirmed that the determination of the maximum growth rate,  $v_{max}$  for the aerobic bacteria was of importance. Next, at the beginning of the experiment, it can be seen that the Mn-(hydr)oxides is dissolved faster than Fe-(hydr)oxides. Thereafter, Mn<sup>2+</sup> and Fe<sup>2+</sup> concentration showed constant values, respectively. To reproduce the variation of both concentrations, it was confirmed that the determinations of the maximum growth rate,  $v_{max}$  for manganese and iron reducers bacteria and the exchange rate,  $\gamma$  and the initial concentrations of

**Table 2** Parameters used for the simulation.

Biochemical parameters	This model	Schäfer <i>et al.</i> (1998b)
Specific volume of biophase ( $n_{bio}$ )	0.02	0.02
Exchange coefficient ( $\alpha$ )	50 day <sup>-1</sup>	50 day <sup>-1</sup>
Exchange coefficient ( $\beta$ )	$5 \times 10^{-3}$ day <sup>-1</sup>	–
Exchange coefficient ( $\gamma$ )	$8 \times 10^{-5}$ day <sup>-1</sup>	$1.1 \times 10^{-3}$ day <sup>-1</sup>
Maximum microbial capacity	–	0.07 mol bacteria-C/1 biophase
Monod constant for organic carbon ( $MC_{OC}$ )	0.1 mmol l <sup>-1</sup>	0.1 mmol l <sup>-1</sup>
Monod constant for oxygen ( $MC_{Oxy}$ )	$1 \times 10^{-5}$ mmol l <sup>-1</sup>	$1 \times 10^{-5}$ mmol l <sup>-1</sup>
Inhibition concentration of denitrifiers against O <sub>2</sub>	–	0.2 mmol l <sup>-1</sup>
Inhibition concentration of Fe(III)-, Mn(IV)-reducers against O <sub>2</sub>	–	0.1 mmol l <sup>-1</sup>
<b>Aerobic bacteria</b>		
Yield coefficient ( $Y$ )	0.1 mol cell-C/mol OC	0.1 mol cell-C/mol OC
Maximum growth rate ( $v_{max}$ )	5 day <sup>-1</sup>	3 day <sup>-1</sup>
Constant decay rate ( $v_{dec}$ )	0.75 day <sup>-1</sup>	0.3 day <sup>-1</sup>
<b>Nitrate reducers</b>		
Yield coefficient ( $Y$ )	0.081 mol cell-C/mol OC	0.92 mol cell-C/mol OC
Maximum growth rate ( $v_{max}$ )	4.05 day <sup>-1</sup>	2.75 day <sup>-1</sup>
Constant decay rate ( $v_{dec}$ )	0.75 day <sup>-1</sup>	0.275 day <sup>-1</sup>
<b>Manganese reducers</b>		
Yield coefficient ( $Y$ )	0.015 mol cell-C/mol OC	0.074 mol cell-C/mol OC
Maximum growth rate ( $v_{max}$ )	0.75 day <sup>-1</sup>	2.2 day <sup>-1</sup>
Constant decay rate ( $v_{dec}$ )	0.113 day <sup>-1</sup>	0.22 day <sup>-1</sup>
<b>Iron reducers</b>		
Yield coefficient ( $Y$ )	0.010 mol cell-C/mol OC	0.003 mol cell-C/mol OC
Maximum growth rate ( $v_{max}$ )	0.5 day <sup>-1</sup>	0.1 day <sup>-1</sup>
Constant decay rate ( $v_{dec}$ )	0.075 day <sup>-1</sup>	0.01 day <sup>-1</sup>



The vertical axis for the above graphs indicates meq l<sup>-1</sup> for Mn<sup>2+</sup>, Fe<sup>2+</sup>, O<sub>2</sub>, V for ORP, and mmol l<sup>-1</sup> for NO<sub>3</sub><sup>-</sup> in order from the left.

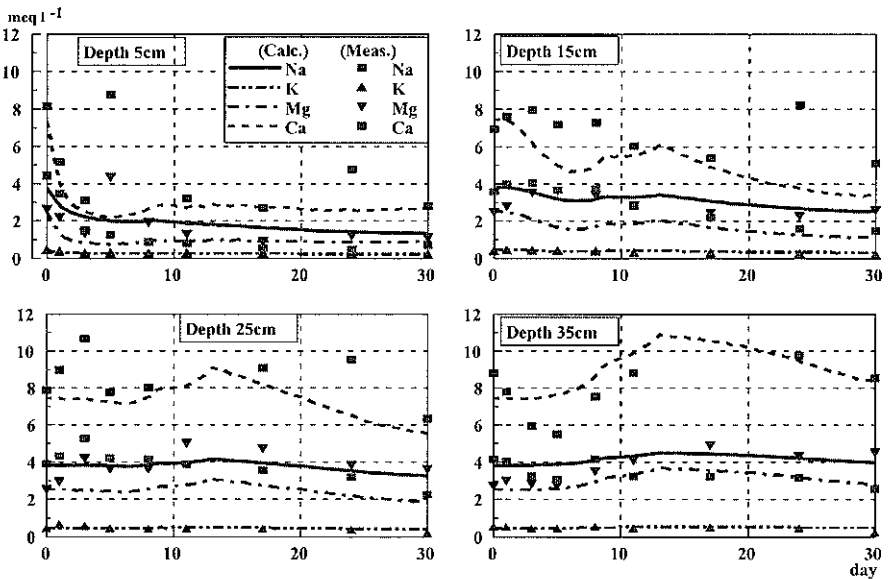


Fig. 2 Comparison of the temporal measured and calculated concentrations of chemical species and the variation of ORP.

MnO<sub>2</sub> and Fe(OH)<sub>3</sub> in the biophase were important. With the rise of Mn<sup>2+</sup> and Fe<sup>2+</sup> concentrations in the pore water, Mg<sup>2+</sup> and Ca<sup>2+</sup> adsorbed on the solid phase appeared. It can be assumed that Mn<sup>2+</sup> and Fe<sup>2+</sup> released by a reduction reaction take part in the cation exchange as exchangeable ions.

## CONCLUSIONS

This paper describes an experiment and the modelling of multicomponent solute transport under redox condition similar to an actual paddy field. Surprisingly,  $Mn^{2+}$  and  $Fe^{2+}$  were detected in the pore water in this experiment. The biochemical reactions and the cation exchange reaction were modelled in the convective–dispersive equation as the sink/source terms. The simulated concentrations of  $O_2$ ,  $NO_3^-$ ,  $Mn^{2+}$ , and  $Fe^{2+}$  approximately agreed with the experimental results. The model was also considered to evaluate the cation exchange reaction which occurred between the pore water and the cations ( $Na^+$ ,  $K^+$ ,  $Mg^{2+}$ ,  $Ca^{2+}$ ) adsorbed on the solid phase. It was found that the  $Mn^{2+}$  and  $Fe^{2+}$  released by reduction reactions played an important role in the cation exchange. The reliability of this model was evaluated by comparing the calculated results with the results of the experiment.

## REFERENCES

- Bear, J. (1972) *Dynamics of Fluid in Porous Media*. Elsevier, New York.
- Kinzelbach, W., Schäfer, W. & Herzer, J. (1991) Numerical modeling of natural and enhanced denitrification processes in aquifer. *Wat. Resour. Res.* **27**(6), 1149–1159.
- Lensing, H. J., Vogt, M. & Herrling, B. (1994) Modeling of biologically mediated redox processes in the subsurface. *J. Hydrol.* **159**, 125–143.
- Matsunaga, T., Karametaxas, G., von Gunten, H. R. & Lichtner, P. C. (1993) Redox chemistry of iron and manganese minerals in river-recharged aquifer: a model interpretation of a column experiment. *Geochimica et Cosmochimica Acta* **57**, 1691–1704.
- Rubin, J. (1983) Transport of reacting solutes in porous media: relation between mathematical nature of problem formulation and chemical nature of reactions. *Wat. Resour. Res.* **19**, 1231–1252.
- Schäfer, D., Schäfer, W. & Kinzelbach, W. (1998a) Simulation of reactive processes related to biodegradation in aquifers. 1. Structure of the three-dimensional reactive transport model. *J. Contam. Hydrol.* **31**, 167–186.
- Schäfer, D., Schäfer, W. & Kinzelbach, W. (1998b) Simulation of reactive processes related to biodegradation in aquifers. 2. Model application to a column study on organic carbon degradation. *J. Contam. Hydrol.* **31**, 187–209.